A Fixed-Grid Finite Element Algebraic Multigrid Approach for Interface Shape Optimization Governed by 2-Dimensional Magnetostatics*

Dalibor Lukáš[1] and J.K. Kraus[2]

[1] Department of Applied Mathematics, VŠB–Technical University of Ostrava, 17. listopadu 15, 708 33 Ostrava–Poruba, Czech Republic
[2] RICAM, Austrian Academy of Sciences, Altenberger Strasse 69, 4040 Linz, Austria

Abstract. The paper deals with a fast computational method for discretized optimal shape design problems governed by 2–dimensional magnetostatics. We discretize the underlying state problem using linear Lagrange triangular finite elements and in the optimization we eliminate the state problem for each shape design. The shape to be optimized is the interface between the ferromagnetic and air domain. The novelty of our approach is that shape perturbations do not affect grid nodal displacements, which is the case of the traditional moving–grid approach, but they are rather mapped to the coefficient function of the underlying magnetostatic operator. The advantage is that there is no additional restriction for the shape perturbations on fine discretizations. However, this approach often leads to a decay of the finite element convergence rate, which we discuss. The computational efficiency of our method relies on an algebraic multigrid solver for the state problem, which is also described in the paper. At the end we present numerical results.

1 Introduction

Shape optimization covers a class of problems in which one looks for an optimal shape of a part of the boundary or interface of a body subjected to a physical field. The optimality means minimization of a given objective functional among admissible shapes. We will restrict ourselves to the case of interface shape optimization with the physics modelled by a linear partial differential equation (PDE). The abstract setting of the problem reads as follows:

$$\min_{(\alpha,u)\in\mathcal{U}_{\rm ad}\times V} \mathcal{I}(\alpha,u) \quad \text{s.t.} \quad A(\alpha)u = b \quad \text{on } V', \tag{1}$$

* This research has been supported by the Czech Grant Agency under the grant GAČR 201/05/P008, by the Czech Ministry of Education under the project MSM6198910027, by the Czech Academy of Science under the project AVČR 1ET400300415, and by the Austrian Science Fund FWF under the project SFB F013.

where $\mathcal{U}_{\rm ad}$ is a nonempty compact subset of admissible piecewise smooth functions α describing some parts of the interface between $\Omega_0(\alpha)$ and $\Omega_1(\alpha)$ which provide a distinct decomposition of a given domain $\Omega \subset \mathbb{R}^2$. Further, $\mathcal{I}$ denotes an objective continuous functional, V is a Hilbert space of functions over Ω with the dual V', $A(\alpha) \in \mathcal{L}(V, V')$ denotes the PDE operator which continuously depends on α, where $\mathcal{L}(V, V')$ consists of linear continuous operators from V to V', $b \in V'$ denotes a physical field source term, and $u \in V$ is the unique solution to the underlying PDE problem.

There is a number of methods solving the problem (1). Let us classify them regarding how they treat the PDE constraint. The following state elimination (nested, black–box) method, cf. [7], is most traditional in shape optimization:

$$\min_{\alpha \in \mathcal{U}_{\rm ad}} \mathcal{I}(\alpha, A(\alpha)^{-1} b).$$

On the other hand, we can prescribe the state equation via a Lagrange multiplier and solve the following nonlinear saddle–point problem

$$\min_{(\alpha,u) \in \mathcal{U}_{\rm ad}} \max_{\lambda \in V} \left\{ \mathcal{I}(\alpha, u) + \langle A(\alpha)u - b, \lambda \rangle_{V' \times V} \right\},$$

where $\langle ., . \rangle_{V' \times V}$ denotes the duality pairing. This so–called one–shot (simultaneous, primal–dual, all–at–once) method is superior in case of topology optimization, smooth dependence of $\mathcal{I}(\alpha, u)$ and $A(\alpha)$ thanks to a sparsity of the Hessian of the Lagrange functional, which allows to use Newton methods, cf. [4, 6].

Another classification of solution methods follows when we take into account the structure of $A(\alpha)$. Without loss of generality, let us think of the 2–dimensional linear magnetostatic state problem, the classical formulation of which is as follows:

$$\begin{cases} -\nu_0 \triangle u_0(x) & & = J(x) & \text{for } x \in \Omega_0(\alpha), \\ & -\nu_1 \triangle u_1(x) & = 0 & \text{for } x \in \Omega_1(\alpha), \\ u_0(x) & -u_1(x) & = 0 & \text{for } x \in \Gamma(\alpha), \\ \nu_0 \nabla u_0(x) \cdot \mathbf{n}_0(\alpha)(x) & -\nu_1 \nabla u_1(x) \cdot \mathbf{n}_0(\alpha)(x) & = 0 & \text{for } x \in \Gamma(\alpha), \\ & u(x) & = 0 & \text{for } x \in \Gamma_{\rm D}, \\ & \frac{\partial u}{\partial n} & = 0 & \text{for } x \in \Gamma_{\rm N}, \end{cases} \tag{2}$$

where $\nu_0 \gg \nu_1 > 0$ denote the reluctivity of the air and ferromagnetics, respectively, J denotes the electric current density, $\Gamma(\alpha) := \partial\Omega_0(\alpha) \cap \partial\Omega_1(\alpha)$ denotes the interface, $\overline{\Gamma_{\rm D}} \cup \overline{\Gamma_{\rm N}}$ is a distinct decomposition of $\partial\Omega$ into the Dirichlet and Neumann part, $\mathbf{n}_0(\alpha)$ denotes the outward unit normal vector to $\Omega_0(\alpha)$ and where u consists of $u|_{\Omega_0(\alpha)} := u_0$ and $u|_{\Omega_1(\alpha)} := u_1$. Then, a straightforward approach is the following weak formulation of (2) in the Sobolev space $V := H^1_{0,\Gamma_{\rm D}} := \{v \in H^1(\Omega) \,:\, v = 0 \text{ on } \Gamma_{\rm D}\}$:

$$\text{Find } u \in V : \int_\Omega \nu(\alpha)(x) \nabla u(x) \nabla v(x)\, dx = \int_\Omega J(x) v(x)\, dx \;\forall v \in V, \tag{3}$$

where $\nu(\alpha)$ consists of $\nu(\alpha)|_{\Omega_0(\alpha)} := \nu_0$ and $\nu(\alpha)|_{\Omega_1(\alpha)} := \nu_1$ and where J is extended to Ω by zero. Another formulation of (2) prescribes the third and

fourth equations of (2), which are called interface conditions, in a weaker sense using the Lagrange formalism again. This might be viewed as a sort of fictitious domain method, cf. [8], or a domain decomposition method. The formulation is as follows: Find $(u_0, u_1, \lambda_{\mathrm{t}}, \lambda_{\mathrm{n}}) \in V_0 \times V_1 \times H^{1/2}(\Gamma(\alpha)) \times H^{1/2}(\Gamma(\alpha))$ as a solution of

$$\begin{pmatrix} A_0 & , & 0 & , \text{sym.} \\ 0 & , & A_1 & , \text{sym.} \\ I(\alpha) & , & -I(\alpha) & , & 0 \\ B_0(\alpha) & , & -B_1(\alpha) & , & 0 \end{pmatrix} \begin{pmatrix} u_0 \\ u_1 \\ \lambda_{\mathrm{t}} \\ \lambda_{\mathrm{n}} \end{pmatrix} = \begin{pmatrix} J \\ 0 \\ 0 \\ 0 \end{pmatrix}, \tag{4}$$

where the saddle–point structure corresponds to the equations 1–4 in (2) such that for $d = 0, 1$ we define $V_d := \{v \in H^1(\Omega) \ : \ v = 0 \text{ on } \Gamma_{\mathrm{D}} \cap \partial\Omega_d(\alpha)\}$, $A_d u_d := -\nu_d \triangle u_d$, $I(\alpha)u_d := u_d|_{\Gamma(\alpha)}$ and $B_d(\alpha)u_d := \nu_d \nabla u_d(x) \cdot \mathbf{n}_0(\alpha)$. The advantage of this approach is that the PDE–operators A_0 and A_1 are independent of the evolving shape. Thus one can approximate (4) via a discretization of a fixed domain and efficient saddle–point solvers [5, 9, 14] can be used. However, the formulation (4) poses a lower–order convergence rate of finite element approximations and the optimization functional is nondifferentiable. Recently, there has been a growing number of applications of discontinuous Galerkin methods, cf. [3, 12], which turned out to be another proper framework for the interface shape optimization.

The optimization method proposed in this paper is based on state elimination. Our treatment of the interface conditions is half the way from the weak formulation (3) to the domain decomposition approach (4). We approximate the weak formulation (3) on a finite element grid that does not follow the shape α and we map the shape perturbations to the coefficient function of the underlying magnetostatic operator.

For solution of discretized state problems (3) we use an algebraic multigrid (AMG) method. AMG methods [1, 13] are known as efficient and robust linear solvers for elliptic boundary-value problems. Our approach is based on the computation of so-called edge matrices, which provide a good starting point for building efficient AMG components, while keeping the set-up costs low [10]. The resulting AMGm solver we are using, see [11], lies in-between classical AMG [13], i.e., strong and weak edges affect the coarsening and the formation of interpolation molecules, and AMG based on element interpolation–so-called AMGe [2], i.e., small-sized neighborhood matrices serve for the computation of the actual interpolation coefficients.

The rest of the paper is organized as follows: in Section 2 we propose the fixed–grid finite element discretization scheme and we discuss its convergence rate, in Section 3 we describe an algebraic multigrid method under consideration and in Section 4 we provide numerical results.

2 Fixed–Grid Finite Element Method

Let $\Omega \subset \mathbb{R}^2$ be a polygonal domain and let $\overline{\Omega} = \overline{\Omega_0(\alpha)} \cup \overline{\Omega_1(\alpha)}$ be its distinct decomposition that is controlled by a piecewise smooth function α such that

$\mathrm{graph}(\alpha) \subset \partial\Omega_0(\alpha) \cap \partial\Omega_1(\alpha)$. The smoothness improves regularity of the state solution and consequently convergence rate of the method as we will see later in this section. We consider the problem (3). Denote by $h > 0$ a discretization parameter and let $\mathcal{T}_h := \{T_i : i = 1, 2, \ldots, m_h\}$ be a shape regular triangulation of Ω that does not take care of α. We approximate V by the following linear Lagrange finite element subspace of V:

$$V_h := \left\{ v_h(x) \in C(\overline{\Omega}) \mid \forall T_i \in \mathcal{T}_h : v_h|_{T_i} \in P^1(T_i) \text{ and } \forall x \in \Gamma_{\mathrm{D}} : v_h(x) = 0 \right\},$$

where $C(\overline{\Omega})$ denotes the space of functions continuous on $\overline{\Omega}$ and $P^1(T)$ denotes the space of linear polynomials over a triangle T. Let us further assume that the source term $J(x)$ is element-wise constant and that the discretization $\mathcal{T}_h$ follows the jumps of J, i.e. $J(x) = J_i$ on each T_i. The linear form of (3) is thus approximated in a conforming way as follows:

$$b_h(v_h) \equiv b(v_h) := \int_\Omega J(x) v_h(x)\, dx = \sum_{T_i \in \mathcal{T}_h} J_i \int_{T_i} v_h(x)\, dx, \quad v_h \in V_h.$$

However, our discretization does not respect the jumps of the coefficient function $\nu(\alpha)(x)$, which leads to a non–conforming discretization of the bilinear form. Let the triangulation be decomposed as follows, see also Fig. 1 (a):

$$\mathcal{T}_h = \mathcal{T}_{h,0}(\alpha) \cup \mathcal{B}_h(\alpha) \cup \mathcal{T}_{h,1}(\alpha),$$

where for $d = 0, 1$ we define $\mathcal{T}_{h,d}(\alpha) := \{T_i \in \mathcal{T}_h \cap \Omega_d(\alpha) \mid T_i \cap \mathrm{graph}(\alpha) = \emptyset\}$ and where $\mathcal{B}_h(\alpha) := \{T_i \in \mathcal{T}_h \mid T_i \cap \mathrm{graph}(\alpha) \neq \emptyset\}$. Then the discretized bilinear form is evaluated as follows:

$$\begin{aligned} a_h(\alpha)(u_h, v_h) \equiv a(\alpha)(u_h, v_h) &:= \int_\Omega \nu(\alpha)(x) \nabla u_h(x) \nabla v_h(x)\, dx \\ = \sum_{T_i \in \mathcal{T}_{h,0}(\alpha)} \nu_0 \int_{T_i} \nabla u_h(x) \nabla v_h(x)\, dx &+ \sum_{T_i \in \mathcal{T}_{h,1}(\alpha)} \nu_1 \int_{T_i} \nabla u_h(x) \nabla v_h(x)\, dx \\ + \sum_{T_i \in \mathcal{B}_h(\alpha)} \frac{\nu_0 |T_i \cap \Omega_0(\alpha)| + \nu_1 |T_i \cap \Omega_1(\alpha)|}{|T_i|} &\int_{T_i} \nabla u_h(x) \nabla v_h(x)\, dx, \quad u_h, v_h \in V_h, \end{aligned}$$

where $|D|$ denotes the area of D.

2.1 Convergence rate

The approximation estimate is given by Céa's lemma:

$$\|u - u_h\|_V \leq C \min_{v_h \in V_h} \|u - v_h\|_V,$$

where $C > 0$ is a generic constant (continuity over ellipticity of the bilinear form) which is independent of h in case of shape regular discretizations. Let $\Pi_h : V \to$

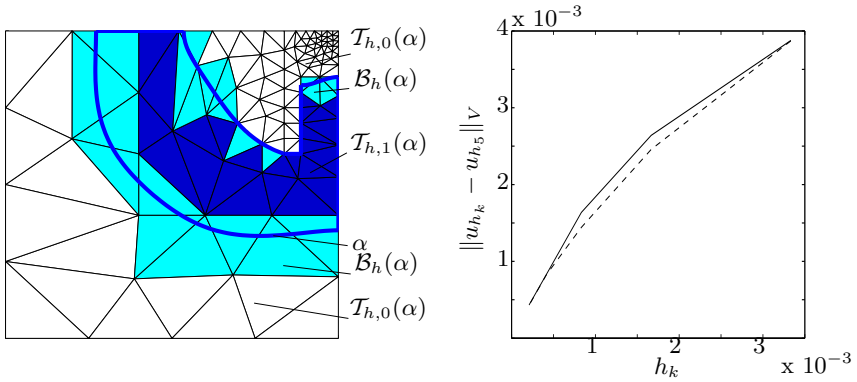

Fig. 1. (a) Decomposition of the discretization controlled by the shape α – only the three inner non-straight curves are controlled, their end points are connected by straight lines; (b) Convergence curve for the fixed–grid approach (solid line) and for the conforming approach (dashed line) computed on 5 levels, where $\|u_{h_k} - u\|_V \approx \|u_{h_k} - u_{h_5}\|_V$ for $k = 0, 1, \ldots, 4$

V_h denote the finite element interpolation operator, e.g. of the Clément–type, and let us choose $v_h := \Pi_h u$. Then, we arrive at the following:

$$\|u - \Pi_h u\|_V^2 \leq \sum_{\substack{T_i \in \mathcal{T}_{h,0}(\alpha) \\ T_i \cap \mathrm{supp}(J) = \emptyset}} \|u - \Pi_h u\|_{H^1(T_i)}^2 + \sum_{\substack{T_i \in \mathcal{T}_{h,0}(\alpha) \\ T_i \subset \mathrm{supp}(J)}} \|u - \Pi_h u\|_{H^1(T_i)}^2$$

$$+ \sum_{T_i \in \mathcal{T}_{h,1}(\alpha)} \|u - \Pi_h u\|_{H^1(T_i)}^2 + \sum_{T_i \in \mathcal{B}_h(\alpha)} \|u - \Pi_h u\|_{H^1(T_i)}^2.$$

Since our discretization respects the jumps of $J(x)$ and does not respect the jumps of $\nu(\alpha)(x)$, the solution u is regular everywhere except for $T_i \in \mathcal{B}_h(\alpha)$. Combining the previous estimates and the standard regularity argument implies that

$$\|u - u_h\|_V \leq C'h + C''h^{-1} \max_{T_i \in \mathcal{B}_h(\alpha)} \|u - \Pi_h u\|_{H^1(T_i)},$$

where the factor h^{-1} is related to the number of elements in $\mathcal{B}_h(\alpha)$. Therefore, the rate of convergence depends on the order of regularity of u across the coefficient jump interface $\Gamma(\alpha)$. Recall that for our shape optimization purposes $\Gamma(\alpha)$ is a smooth curve.

The convergence rate remains an open question. In order to indicate it, we refer to Fig. 1 (b), where we compare the convergence curve for the case of conforming discretization (respecting the coefficient jump) to the fixed–grid case. We can see that both the curves slightly deteriorate from the linear convergence, but the conforming discretization does not improve much. We used uniform refinement of the grid in Fig. 1 (a), where for levels $k = 0, 1, \ldots, 5$ the number of elements/number of nodes are respectively 317/186, 1268/688, 5072/2643, 20288/10357, 81152/41001 and 324608/163153 and where the corresponding discretizatization parameter is $h_k \approx 0.0033/2^k$.

3 Algebraic multigrid

We are solving the discretized state problem using an algebraic multigrid method that agrees with classical AMG [13], except for the coarse-grid selection and the interpolation component, which are controlled by edge matrices in case of our approach, see [11]. Note that a novelty here is an application to the fixed–grid shape optimization.

One can also view this as involving an auxiliary problem–the one determined by the edge matrices–in the coarsening process. The coarse-grid matrices, however, are still computed via the usual Galerkin triple matrix product, i.e., $A_{k+1} = P_k^T A_k P_k$ at all levels $k = 0, 1, \ldots, \ell - 1$.

The basic idea is to construct suitable small-sized computational molecules from edge matrices and to choose the interpolation coefficients in such a way that they provide a local minimum energy extension with respect to the considered interpolation molecule. Assuming that "weak" and "strong" edges have been identified, the coarse grid has been selected, and a set of edge matrices is available, one defines a so-called interpolation molecule for every f-node i (to which interpolation is desired), cf. [11]:

$$M(i) := \sum_{k \in \mathcal{S}_i^c} E_{ik} + \sum_{j \in \mathcal{N}_i^f \colon \exists k \in \mathcal{S}_i^c \cap \mathcal{N}_j} E_{ij} + \sum_{k \in \mathcal{S}_i^c \cap \mathcal{N}_j \colon j \in \mathcal{N}_i^f} E_{jk}, \tag{5}$$

where the following symbols respectively denote $\mathcal{D}_f$ fine nodes (f-nodes), $\mathcal{D}_c$ coarse nodes (c-nodes), $\mathcal{D} := \mathcal{D}_f \cup \mathcal{D}_c$ all nodes, $\mathcal{N}_i$ direct neighbors of node i, $\mathcal{N}_i^f := \mathcal{N}_i \cap \mathcal{D}_f$ fine direct neighbors, $\mathcal{S}_i$ strongly connected direct neighbors of node i and $\mathcal{S}_i^c := \mathcal{S}_i \cap \mathcal{D}_c$ strongly connected coarse direct neighbors. This molecule arises from assembling all edge matrices E_{pq} associated with three types of edges: The first sum corresponds to the strong edges connecting node i to some coarse direct neighbor k (interpolatory edges). The second sum represents edges connecting the considered f-node i to any of its fine direct neighbors j being directly connected to at least one c-node k that is strongly connected to node i. Finally, the last sum in (5) corresponds to these latter mentioned connections (edges) between fine direct neighbors j and strongly connected coarse direct neighbors k of node i.

The interpolation molecule (5) then serves for the computation of the actual interpolation weights: For a given f-node i let

$$M(i) = M = \begin{pmatrix} M_{ff} & M_{fc} \\ M_{cf} & M_{cc} \end{pmatrix} \tag{6}$$

be the interpolation molecule where the 2×2 block structure in (6) corresponds to the n_M^f f-nodes and the n_M^c c-nodes the molecule is based on. Consider now the small-sized (local) interpolation matrix

$$P_M = P = \begin{pmatrix} P_{fc} \\ I_{cc} \end{pmatrix}$$

associated with (6). Since M (for the problems under consideration) is symmetric and positive semidefinite (SPSD) we may apply the following concept [2]: For any vector $\mathbf{e}^T = (\mathbf{e}_f^T, \mathbf{e}_c^T) \perp \ker(M)$ we denote by

$$\mathbf{d}_f := \mathbf{e}_f - P_{fc}\mathbf{e}_c \tag{7}$$

the defect of (local) interpolation. With the objective of an energy minimizing coarse basis we choose P_{fc} to be the argument that minimizes

$$\max_{\mathbf{e}\perp\ker(M)} \frac{(\mathbf{e}_f - P_{fc}\mathbf{e}_c)^T(\mathbf{e}_f - P_{fc}\mathbf{e}_c)}{\mathbf{e}^T M \mathbf{e}}.$$

Using (7) and $G := P_{fc}^T M_{ff} P_{fc} + P_{fc}^T M_{fc} + M_{cf} P_{fc} + M_{cc}$ one finds

$$\begin{aligned}
&\min_{P_{fc}} \max_{\mathbf{d}_f, \mathbf{e}_c} \frac{\mathbf{d}_f^T \mathbf{d}_f}{\begin{pmatrix} \mathbf{d}_f + P_{fc}\mathbf{e}_c \\ \mathbf{e}_c \end{pmatrix}^T \begin{pmatrix} M_{ff} & M_{fc} \\ M_{cf} & M_{cc} \end{pmatrix} \begin{pmatrix} \mathbf{d}_f + P_{fc}\mathbf{e}_c \\ \mathbf{e}_c \end{pmatrix}} \\
&= \min_{P_{fc}} \max_{\mathbf{d}_f} \frac{\mathbf{d}_f^T \mathbf{d}_f}{\mathbf{d}_f^T \left[M_{ff} - (M_{ff}P_{fc} + M_{fc}) G^{-1} (P_{fc}^T M_{ff} + M_{cf}) \right] \mathbf{d}_f}.
\end{aligned} \tag{8}$$

Assuming that M_{ff} and G both are SPD the denominator of (8) for an arbitrary vector $\mathbf{d}_f$ is maximized and thus the minimum is attained for

$$P_{fc} := -M_{ff}^{-1} M_{fc}, \tag{9}$$

which results in $1/(\lambda_{\min}(M_{ff}))$. This motivates to choose the interpolation coefficients for node i to equal the entries in the corresponding row of (9).

4 Numerical results

We consider a problem of optimal shape design of pole heads of a direct current (DC) electromagnet, which is depicted in Fig. 2 (a), while we simplify the geometry so that only two opposite pole heads and coils are present. The goal is to achieve homogeneous magnetic field in a small square Ω_{m} in the middle among the pole heads, which is evaluated by the following objective functional:

$$\mathcal{I}(u) := \frac{1}{2|\Omega_{\mathrm{m}}|} \int_{\Omega_{\mathrm{m}}} \|\mathrm{curl}(u(x)) - B^{\mathrm{avg}}(u(x))\mathbf{n}_{\mathrm{m}}\|^2 \, dx + \frac{\varepsilon_u}{2|\Omega|} \int_{\Omega} \|\nabla u\|^2 \, dx,$$

where $\mathrm{curl}(u) := (\partial u/\partial x_2, -\partial u/\partial x_1)$ is the magnetic flux density, $\Omega := (-0.2, 0)^2$ (in meters), $\Omega_{\mathrm{m}} := (-0.01, 0)^2$, $\varepsilon_u := 10^{-3}$ introduces a regularization in $H^1(\Omega)$ and where

$$B^{\mathrm{avg}}(u(x)) := \frac{1}{|\Omega_{\mathrm{m}}|} \int_{\Omega_{\mathrm{m}}} \mathrm{curl}(u(x))\mathbf{n}_{\mathrm{m}} \, dx.$$

An admissible shape α consists of 3 Bézier curves that are the non–straight curves depicted in Fig. 1 (a). For them we consider 7, 4 and 7 design control parameters (18 in total), respectively, and we further introduce two other shapes α_{l} and α_{u}, which are again triples of such Bézier curves, that form box constraints for the set of admissible shapes $\mathcal{U}_{\mathrm{ad}}$. This optimization is subjected to the state equation (3), which we denote by $u(\alpha)$.

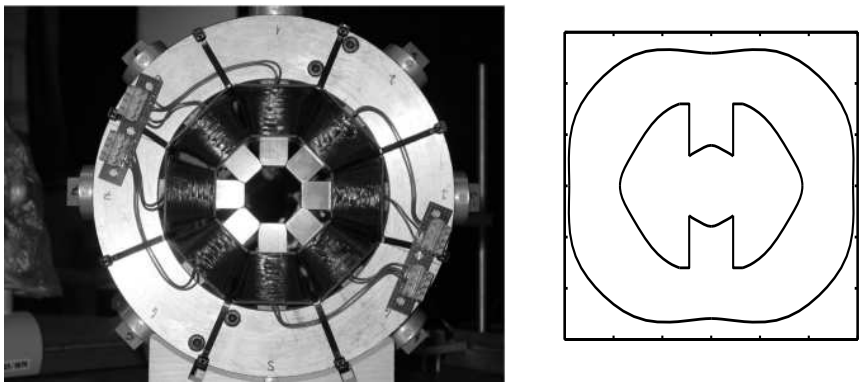

Fig. 2. (a) Original electromagnet; (b) Optimized design

The optimization algorithm includes a steepest descent method, a projection to the box constraints and a numerical differentiation for calculation of $\nabla_\alpha \mathcal{I}(u(\alpha)(x))$. The optimized design is depicted in Fig. 2 (b). For the discretization of the state equation we used the finite element fixed–grid approach of Section 2 and the AMG method of Section 3, which was accelerated by the preconditioned conjugate gradients method(PCG). We set up the AMG preconditioner only for the first system at each discretization level and used this setup at the level as a preconditioner for all the other forthcoming systems, which are perturbed by different shapes via the fixed–grid approach. Both the PCG and optimization relative precision were 10^{-8}. The preliminary numerical results are presented in Table 1. The AMG preconditioner certainly deteriorates for perturbed systems, because it is not re–setup, which is a cheap operation that we will use in the next version. However, we could by far not achieve such moderate decay of AMG for example as in the case of geometric multigrid solver, where the iterations grows easily up to hundreds.

References

1. A. Brandt: Algebraic multigrid theory: the symmetric case. Appl. Math. Comput. 19 (1986), 23–56.
2. M. Brezina, A.J. Cleary, R.D. Falgout, V.E. Henson, J.E. Jones, T.A. Manteuffel, S.F. McCormick, and J.W. Ruge: Algebraic multigrid based on element interpolation (AMGe). SIAM J. Sci. Comput. 22 (2000), 1570-1592.

discretization level	number of elements	number of nodes	number of AMG levels	PCG iterations	optimization iterations
0	317	186	2	6	4
1	9649	4985	4	10–15	5
2	34658	17629	6	15–43	2
3	134292	67721	8	29–61	4

Table 1. Numerical results

3. Arnold, D., Brezzi, F., Cockburn, B, and Marini, L.: Unified analysis of discontinuous Galerkin methods for elliptic problems, SIAM J. Numer. Anal. **39** (2002) 1749–1779
4. Borzi, A.: Multigrid Methods for Optimality Systems, habilitation thesis, TU Graz (2003)
5. Bramble, J. H., Pasciak, J. E., Vassilev, A. T.: Analysis of the inexact Uzawa algorithm for saddle point problems, SIAM J. Numer. Anal. **34** (1997) 1072–1092
6. Dreyer, T., Maar, B., Schulz, V.: Multigrid optimization in applications, J. Comp. Appl. Math. **120** (2000) 67–84
7. Haslinger J., Neittaanmäki P.: Finite Element Approximation for Optimal Shape, Material and Topology Design. Wiley, Chinchester (1997)
8. Haslinger, J. and Klarbring, A.: Fictitious domain/mixed finite element approach for a class of optimal shape design problems, RAIRO, Modélisation Math. Anal. Numér. **29** (1995) 435–450
9. Lukáš, D., Dostál, Z.: Optimal multigrid preconditioned semi–monotonic augmented Lagrangians Applied to the Stokes Problem, Num. Lin. Alg. Appl. (submitted)
10. Kraus, J.K.: On the utilization of edge matrices in algebraic multigrid. In Proceedings of the 5th International Conference, LSSC 2005, I. Lirkov, S. Margenov, and J. Waśniewski, eds., Springer LNCS 3743, 121–129, 2006.
11. Kraus, J.K., Schicho, J.: Algebraic multigrid based on computational molecules, 1: Scalar elliptic problems. Computing **77** (2006) 57–75.
12. Rivière, B. and Bastian, P.: Discontinuous Galerkin methods for two–phase flow in porous media, Research report of Interdisciplinary Center for Scientific Computing, University Heidelberg (2004)
13. J.W. Ruge and K. Stüben: Efficient solution of finite difference and finite element equations by algebraic multigrid (AMG). In: Multigrid Methods for Integral and Differential Equations, D.J. Paddon and H. Holstein, eds., The Institute of Mathematics and Its Applications Conference Series, Clarendon Press, Oxford, 1985, 169-212.
14. Schöberl, J., Zulehner, W.: Symmetric indefinite preconditioners for saddle point problems with applications to PDE–constrained optimization problems, SFB Report 2006-19, University Linz (2006)